Time Series Control Charts in the Presence of Model Uncertainty

Daniel W. Apley
Assistant Professor,
Mem., ASME
Department of Industrial Engineering,
Texas A&M University,
College Station, TX 77843-3131
e-mail: apley@tamu.edu

Time series control charts are popular methods for statistical process control of autocorrelated processes. In order to implement these methods, however, a time series model of the process is required. Since time series models must always be estimated from process data, model estimation errors are unavoidable. In the presence of modeling errors, time series control charts that are designed under the assumption of a perfect model may have an actual in-control average run length that is substantially shorter than desired. This paper presents a method for incorporating model uncertainty information into the design of time series control charts to provide a level of robustness with respect to modeling errors. The focus is on exponentially weighted moving average charts and Shewhart individual charts applied to the time series residuals. [DOI: 10.1115/1.1510520]

1 Introduction

Statistical process control (SPC) techniques are widely used for monitoring and improving quality in industrial processes. Traditional SPC is based on the assumption that process data are independent. Advances that have occurred in the areas of measurement and data collection technology, however, result in the common scenario where large amounts of highly autocorrelated in-process measurement data are available for process monitoring and diagnosis (Montgomery and Woodall [1]). It is well known that the in-control average run length (ARL) of traditional SPC methods like CUSUM, $\bar{X}$, and EWMA charts may be much shorter than intended when data are autocorrelated (Johnson and Bagshaw [2]; Vasilopoulos and Stamboulis [3]). As a result, there has been significant research in recent years on designing SPC procedures suitable for autocorrelated processes (see, e.g., Montgomery and Woodall [1], Lu and Reynolds [4], and the references therein).

Some of the most widely investigated methods for SPC of autocorrelated processes are time series control charts, also referred to as residual-based control charts. Typically, the process data x_t (t is a time index) are assumed to follow an autoregressive moving-average (ARMA) model of the form

$$x_t-\phi_1x_{t-1}-\phi_2x_{t-2}-\cdots-\phi_px_{t-p} = a_t-\theta_1a_{t-1}-\theta_2a_{t-2}-\cdots-\theta_qa_{t-q}, \quad (1)$$

where the ϕ's and θ's are constant parameters, p is the autoregressive (AR) order, q is the moving average (MA) order, and a_t is assumed to be an identically independently distributed (i.i.d.) zero-mean random sequence that follows a normal distribution with variance σ_a^2. Using the backward shift operator B, Eq. (1) can be written as

$$x_t=\frac{\Theta(B)}{\Phi(B)}a_t, \quad (2)$$

where $\Theta(B)=1-\theta_1B-\theta_2B^2-\ldots-\theta_qB^q$ and $\Phi(B)=1-\phi_1B-\phi_2B^2-\ldots-\phi_pB^p$.

The basic idea behind residual-based charts is to directly monitor the residuals (i.e., the one-step-ahead prediction errors) of the time series model, generated via $e_t=\Theta^{-1}(B)\Phi(B)x_t$. From Eq. (2), it follows that after the initial transients have died out, e_t is exactly the i.i.d. sequence a_t. Thus, the residuals are uncorrelated, and traditional control charts can be applied with well understood in-control run length properties. Various research (see e.g., Alwan and Roberts [5], Apley and Shi [6], Berthouex, Hunter, and Pallesen [7], Dooley and Kapoor [8], Dooley, Kapoor, Dessouky, and DeVor [9], English, Krishnamurthi, and Sastri [10], Lin and Adams [11], Montgomery and Mastrangelo [12], Notohardjono and Ermer [13], Runger, Willemain, and Prabhu [14], Superville and Adams [15], Vander Wiel [16], and Wardell, Moskowitz, and Plante [17]) has investigated applying Shewhart, CUSUM, EWMA, and other types of control charts to the residuals.

In practice, the ARMA model must always be estimated from process data. Let $\{\hat{\phi}_i\}_{i=1}^p$, $\{\hat{\theta}_i\}_{i=1}^q$, and $\hat{\sigma}_a^2$ be estimates of the ARMA parameters, and define $\hat{\Phi}(B)$ and $\hat{\Theta}(B)$ to be the AR and MA polynomials constructed from the estimated parameters. For simplicity, it is assumed throughout this paper that p and q are known. The residuals are generated using the estimated model via

$$e_t=\frac{\hat{\Phi}(B)}{\hat{\Theta}(B)}x_t=\frac{\hat{\Phi}(B)\Theta(B)}{\hat{\Theta}(B)\Phi(B)}a_t. \quad (3)$$

With estimation errors, the residuals follow the ARMA($p+q,p+q$) model (3) and are no longer i.i.d. Residual autocorrelation due to modeling errors can have large impact on the in-control ARL of residual-based charts, as demonstrated empirically in Adams and Tseng [18], Apley and Shi [6], and Lu and Reynolds [4].

To illustrate why, suppose a residual-based EWMA chart is used to monitor an ARMA process. The residual-based EWMA statistic is defined recursively via

$$z_t=(1-\lambda)z_{t-1}+\lambda e_t, \quad (4)$$

where $0<\lambda\leq 1$ is the user-specified EWMA parameter (Montgomery [19]). For a specified λ, the typical EWMA design procedure when the model is assumed perfect is to set the control limits for z_t at (Lu and Reynolds [4])

$$\pm L\sigma_{Z,0}=\pm L\hat{\sigma}_a\sqrt{\frac{1-\nu}{1+\nu}}, \quad (5)$$

where the constant L is chosen to provide a desired in-control ARL, $\nu=1-\lambda$, and $\sigma_{z,0}^2=\hat{\sigma}_a^2(1-\nu)/(1+\nu)$ is the variance of z_t (in the steady-state, after initial transients have died out) under the assumption that there are no modeling errors. Tables provided in Lucas and Saccucci [20] give the L values that result in several different in-control ARLs for various choices of λ.

Since with modeling errors the residuals will be autocorrelated, the actual variance of z_t may differ considerably from $\sigma_{z,0}^2$. Combining Eq. (3) and Eq. (4), it follows that z_t obeys the ARMA($p+q+1,p+q$) model

$$z_t=\frac{(1-\nu)\hat{\Phi}(B)\Theta(B)}{(1-\nu B)\hat{\Phi}(B)\Phi(B)}a_t. \quad (6)$$

Contributed by the Manufacturing Engineering Division for publication in the JOURNAL OF MANUFACTURING SCIENCE AND ENGINEERING. Manuscript received September 2000; Revised January 2002. Associate Editor: S. J. Hu.

For a given set of parameters and parameter estimates, the variance of z_t may be calculated using the impulse response method (Box et al. [21]) discussed in Section 3. If the parameter estimates are such that the residuals are positively autocorrelated, the variance of z_t will be larger than $\sigma_{z,0}^2$ and the resulting in-control ARL will be shorter than desired, possibly by a substantial amount (Adams and Tseng [18]).

Viewing the parameter estimates as random, the EWMA variance is itself a random variable. Let σ_z^2 denote the expected value of the EWMA variance, where the expectation is with respect to the distribution of the random parameter estimates. It will be shown that σ_z^2 is a function of the covariance matrix of $\{\hat{\phi}_i\}_{i=1}^p$ and $\{\hat{\theta}_i\}_{i=1}^q$, an estimate of which is typically available as a measure of model uncertainty when ARMA parameters are estimated (Box et al. [21]). In analogy with (5), the basic idea of this paper is to use

$$\pm L\sigma_z, \tag{7}$$

as control limits for the residual-based EWMA. As will be shown, σ_z^2 is always larger than $\sigma_{z,0}^2$ because of the uncertainty involved in estimating ARMA models. Consequently, the control limits (7) are wider than the traditional control limits (5) that are used when models are assumed perfect. In this sense, the proposed method safeguards against an undesirably short in-control ARL due to ARMA modeling errors. Although the sensitivity of residual-based charts to modeling errors is well known, the proposed method is the first that incorporates model uncertainty information into the control chart design to provide such a safeguard.

The majority of the technical content of the paper is devoted to developing an expression for σ_z^2, to be used in (7). The focus is on residual-based EWMA charts for first-order ARMA processes, although results for arbitrary-order ARMA processes are presented in Section 3. The results also apply to the Shewhart individual chart, which is a special case of the EWMA chart with $\lambda = 1.0$.

2 Representing Model Uncertainty

Suppose x_t follows a stable, invertible ARMA(p,q) model (2), p and q are known, and the model parameters are estimated from n observations of x_t. Define the parameter vector as $\boldsymbol{\gamma} = [\phi_1 \phi_2 \ldots \phi_p \theta_1 \theta_2 \ldots \theta_q]^T$. Similarly, define $\hat{\boldsymbol{\gamma}}$ to be the estimated parameter vector and $\tilde{\boldsymbol{\gamma}} = \hat{\boldsymbol{\gamma}} - \boldsymbol{\gamma}$ to be the error. Most of the widely used estimation methods, such as nonlinear least squares and exact or approximate maximum likelihood methods, produce similar results and are largely based on minimizing the sum of the squares of the model residuals (Box et al. [21]). For these methods, an approximate expression (that is asymptotically exact) for the covariance matrix of $\hat{\boldsymbol{\gamma}}$ is (Box et al. [21])

$$\Sigma_\gamma = \frac{\sigma_a^2}{n}\Sigma_W^{-1},$$

where Σ_W is the covariance matrix of the random vector $\mathbf{w}_t$, defined as $\mathbf{w}_t = [u_t u_{t-1} \ldots u_{t-p+1} v_t v_{t-1} \ldots v_{t-q+1}]^T$. The random processes u_t and v_t are defined via

$$u_t = \frac{1}{\Phi(B)} a_t, \quad \text{and}$$

$$v_t = -\frac{1}{\Theta(B)} a_t.$$

It can be shown (Box et al. [21]) that for the special cases of AR(1), MA(1), and ARMA(1,1) processes, the covariance matrices are

$$\Sigma_\gamma = \frac{1-\phi_1^2}{n}: \text{ for AR(1)} \tag{8}$$

$$\Sigma_\gamma = \frac{1-\theta_1^2}{n}: \text{ for MA(1)} \tag{9}$$

$$\Sigma_\gamma = \frac{(1-\phi_1\theta_1)}{n(\phi_1-\theta_1)^2}\begin{bmatrix} (1-\phi_1^2)(1-\phi_1\theta_1) & (1-\phi_1^2)(1-\theta_1^2) \\ (1-\phi_1^2)(1-\theta_1^2) & (1-\theta_1^2)(1-\phi_1\theta_1) \end{bmatrix}: \text{ for ARMA(1,1,)} \tag{10}$$

These expressions for Σ_γ provide the model uncertainty representation that will be used when determining the EWMA variance σ_z^2 in Section 4.

3 The Effects of Model Uncertainty on the EWMA Variance for General ARMA Processes

From Eq. (6), the variance of z_t clearly depend on $\hat{\boldsymbol{\gamma}}$. Denote the conditional variance of z_t, given $\hat{\boldsymbol{\gamma}}$, as $\sigma_{z|\hat{\gamma}}^2 = E[z_t^2|\hat{\boldsymbol{\gamma}}]$, where $E[\cdot]$ is the expectation operator. The unconditional variance of z_t can be written as

$$\sigma_z^2 = E[z_t^2] = E[E[z_t^2|\hat{\gamma}]] = E[\sigma_{z|\hat{\gamma}}^2]$$

The strategy for finding $\sigma_{z|\hat{\gamma}}^2$ and σ_z^2 is to linearize the model (6) about $\hat{\Phi}(B) = \Phi(B)$ and $\hat{\Theta}(B) = \Theta(B)$. Linearizing gives

$$\begin{aligned}
&\frac{(1-\nu)\hat{\Phi}(B)\Theta(B)}{(1-\nu B)\hat{\Theta}(B)\Phi(B)} \\
&\quad = \left[\frac{(1-\nu)\Theta(B)}{(1-\nu B)\Phi(B)}\right]\left[\frac{\Phi(B)+\tilde{\Phi}(B)}{\Theta(B)+\tilde{\Theta}(B)}\right] \\
&\quad \cong \left[\frac{(1-\nu)\Theta(B)}{(1-\nu B)\Phi(B)}\right]\left[\frac{\Phi(B)}{\Theta(B)} + \frac{\tilde{\Phi}(B)}{\Theta(B)} - \frac{\Phi(B)\tilde{\Theta}(B)}{\Theta^2(B)}\right] \\
&\quad = (1-\nu)\left[\frac{1}{1-\nu B} + \frac{\tilde{\Phi}(B)}{(1-\nu B)\Phi(B)} - \frac{\tilde{\Theta}(B)}{(1-\nu B)\Theta(B)}\right],
\end{aligned} \tag{11}$$

where $\tilde{\Phi}(B) = \hat{\Phi}(B) - \Phi(B) = -\tilde{\phi}_1 B - \tilde{\phi}_2 B^2 - \ldots - \tilde{\phi}_p B^p$, and $\tilde{\Theta}(B) = \hat{\Theta}(B) - \Theta(B) = -\tilde{\theta}_1 B - \tilde{\theta}_2 B^2 - \ldots - \tilde{\theta}_q B^q$. $\tilde{\phi}_i = \hat{\phi}_i - \phi_i$ and $\tilde{\theta}_i = \hat{\theta}_i - \theta_i$ are defined as the parameter estimation errors. Note that the third line of (11) involves the linearization of the *operator* $\hat{\Theta}^{-1}(B)\hat{\Phi}(B)$ that maps the space of infinite random sequences into itself. This operator can also be viewed as a function of the ARMA parameter estimates that is continuously differentiable (where continuity is with respect to any suitable operator norm) at $\hat{\phi}_i = \phi_i$ and $\hat{\theta}_i = \theta_i$ via the assumption of a stable, invertible ARMA model. Differentiating the first line of (11) with respect to each of the ARMA parameter estimates and then substituting the definition of $\tilde{\Phi}(B)$ and $\tilde{\Theta}(B)$ into the result yields the third line of (11).

Let g_j, $j = 0, 1, 2, \ldots$ denote the coefficients of the impulse response function (Box et al. [21]) of the term in brackets in Eq. (11), i.e.,

$$\left[\frac{1}{1-\nu B} + \frac{\tilde{\Phi}(B)}{(1-\nu B)\Phi(B)} - \frac{\tilde{\Theta}(B)}{(1-\nu B)\Theta(B)}\right] = \sum_{j=0}^{\infty} g_j B^j. \tag{12}$$

The linearized approximation of z_t becomes

$$z_t \cong (1-\nu)\left[\sum_{j=0}^{\infty} g_j B^j\right] a_t = (1-\nu)\sum_{j=0}^{\infty} g_j a_{t-j},$$

where the impulse response coefficients are random variables that depend on the random $\tilde{\boldsymbol{\gamma}}$, in addition to $\boldsymbol{\gamma}$ and ν. The conditional and unconditional variance of z_t become

$$\sigma^2_{z|\hat{\gamma}} \cong (1-\nu)^2\sigma_a^2 \sum_{j=0}^{\infty} g_j^2, \text{ and}$$

$$\sigma_z^2 \cong E[\sigma^2_{z|\hat{\gamma}}] = (1-\nu)^2\sigma_a^2 \sum_{j=0}^{\infty} E[g_j^2]. \tag{13}$$

Since $\tilde{\Phi}(B)$ and $\tilde{\Theta}(B)$ only appear in the numerators of the terms in Eq. (12), each coefficient g_j will be a linear function of $\tilde{\boldsymbol{\gamma}}$. Consequently, each g_j^2 will be a quadratic function of $\tilde{\boldsymbol{\gamma}}$, so that Eq. (13) could be expressed solely in terms of ν, σ_a^2, $\boldsymbol{\gamma}$, and Σ_γ. Appendix B describes a numerical procedure for calculating σ_z^2 for arbitrary order ARMA models. Much of the remainder of this paper focuses on the special cases of AR(1), MA(1), and ARMA(1, 1) processes, for which relatively simple closed-form expressions for σ_z^2 can be derived.

4 Results for First-Order ARMA Processes

For ARMA(1, 1) processes, Eq. (12) becomes

$$\left[\frac{1}{1-\nu B} - \frac{\tilde{\phi}B}{(1-\nu B)(1-\phi B)} + \frac{\tilde{\theta}B}{(1-\nu B)(1-\theta B)}\right] = \sum_{j=0}^{\infty} g_j B^j, \tag{14}$$

where the subscript on the ARMA parameters has been dropped for convenience. In Appendix A it is shown that after finding the impulse response coefficients for Eq. (14), the EWMA variance for ARMA(1, 1) processes becomes

$$\sigma_z^2 \cong \sigma_a^2\left(\frac{1-\nu}{1+\nu}\right)\left[1 + \frac{\Sigma_\phi}{1-\phi^2}\left(\frac{1+\nu\phi}{1-\nu\phi}\right) + \frac{\Sigma_\theta}{1-\theta^2}\left(\frac{1+\nu\theta}{1-\nu\theta}\right) - \frac{2\Sigma_{\phi\theta}}{1-\phi\theta}\left(\frac{1-\nu^2\phi\theta}{(1-\nu\phi)(1-\nu\theta)}\right)\right]. \tag{15}$$

Σ_ϕ, Σ_θ, and $\Sigma_{\phi\theta}$ denote the variance of $\hat{\phi}$, the variance of $\hat{\theta}$, and the covariance between $\hat{\phi}$ and $\hat{\theta}$, respectively, and are the elements of the matrix Σ_γ.

Substituting Σ_γ from Eq. (10) into Eq. (15) gives

$$\sigma_z^2 \cong \sigma_a^2\left(\frac{1-\nu}{1+\nu}\right)\left[1 + \frac{(1-\phi\theta)^2(1+\nu\phi)}{n(\phi-\theta)^2(1-\nu\phi)} + \frac{(1-\phi\theta)^2(1+\nu\theta)}{n(\phi-\theta)^2(1-\nu\theta)} - \frac{2(1-\phi^2)(1-\theta^2)(1-\nu^2\phi\theta)}{n(\phi-\theta)^2(1-\nu\phi)(1-\nu\theta)}\right].$$

Since $2(1-\nu^2\phi\theta)(1-\nu\phi)^{-1}(1-\nu\theta)^{-1} = (1+\nu\phi)(1-\nu\phi)^{-1} + (1+\nu\theta)(1-\nu\theta)^{-1}$, the term in brackets simplifies to

$$\left[1 + \left(\frac{1+\nu\phi}{1-\nu\phi} + \frac{1+\nu\theta}{1-\nu\theta}\right)\frac{(1-\phi\theta)^2 - (1-\phi^2)(1-\theta^2)}{n(\phi-\theta)^2}\right] = \left[1 + \frac{1}{n}\left(\frac{1+\nu\phi}{1-\nu\phi} + \frac{1+\nu\theta}{1-\nu\theta}\right)\right]$$

Thus, the EWMA variance for ARMA(1, 1) processes becomes

$$\sigma_z^2 \cong \sigma_a^2\left(\frac{1-\nu}{1+\nu}\right)\left[1 + \frac{1+\nu\phi}{n(1-\nu\phi)} + \frac{1+\nu\theta}{n(1-\nu\theta)}\right] \tag{16}$$

Note that Eq. (10), and thus Eq. (16), is not valid for $\phi = \theta$. This is a trivial case, however, since an ARMA(1, 1) model with $\phi = \theta$ is equivalent to $x_t = a_t$.

For AR(1) and MA(1) processes, the results are similar. Substituting Eq. (8) into Eq. (15) with $\Sigma_\theta, = \Sigma_{\phi\theta} = \theta = 0$, the EWMA variance for AR(1) processes becomes

$$\sigma_z^2 \cong \sigma_a^2\left(\frac{1-\nu}{1+\nu}\right)\left[1 + \frac{1+\nu\phi}{n(1-\nu\phi)}\right]. \tag{17}$$

Substituting Eq. (9) into Eq. (15) with $\Sigma_{\phi,} = \Sigma_{\phi\theta} = \phi = 0$, the EWMA variance for MA(1) processes becomes

Table 1 EWMA control limits with and without consideration of model uncertainty, for various λ, n $\hat{\phi}$, and $\hat{\theta}$

λ	n	$\hat{\phi}$	$\hat{\theta}$	$L\sigma_{z,0}$	$L\sigma_z$
0.05	50	0.95	0.7	0.419	0.511
0.05	100	0.95	0.7	0.419	0.467
0.05	200	0.95	0.7	0.419	0.444
0.05	50	0.95	0.4	0.419	0.502
0.05	100	0.95	0.4	0.419	0.462
0.05	200	0.95	0.4	0.419	0.441
0.05	50	0.8	0.7	0.419	0.468
0.05	100	0.8	0.7	0.419	0.444
0.05	200	0.8	0.7	0.419	0.432
0.05	50	0.8	0.4	0.419	0.457
0.05	100	0.8	0.4	0.419	0.439
0.05	200	0.8	0.4	0.419	0.429
0.10	50	0.95	0.7	0.646	0.748
0.10	100	0.95	0.7	0.646	0.699
0.10	200	0.95	0.7	0.646	0.673
0.10	50	0.95	0.4	0.646	0.736
0.10	100	0.95	0.4	0.646	0.692
0.10	200	0.95	0.4	0.646	0.669
0.10	50	0.8	0.7	0.646	0.710
0.10	100	0.8	0.7	0.646	0.679
0.10	200	0.8	0.7	0.646	0.662
0.10	50	0.8	0.4	0.646	0.697
0.10	100	0.8	0.4	0.646	0.672
0.10	200	0.8	0.4	0.646	0.659

$$\sigma_z^2 \cong \sigma_a^2\left(\frac{1-\nu}{1+\nu}\right)\left[1 + \frac{1+\nu\theta}{n(1-\nu\theta)}\right]. \tag{18}$$

Since the true parameters are unknown, these expressions for σ_z^2 cannot be directly used in the control limits $\pm L\sigma_z$ from (7). The recommended procedure is to substitute the parameter estimates for their true values in Eq. (16), (17), or (18). L can be selected using existing methods (e.g., Table 4 of Lucas and Saccucci [20] or the Markov chain approach described in Lu and Reynolds [4]), based on λ and the desired in-control ARL. By inspection of Eq. (16) through (18), it is clear that σ_z^2 is strictly larger than the EWMA variance $\sigma_{z,0}^2 = \sigma_a^2(1-\nu)/(1+\nu)$ that results when the model is assumed perfect. Eq. (*B*.2) in Appendix B demonstrates that this is also true for higher-order ARMA models. Consequently, the end result of considering model uncertainty in the design procedure is to use wider control limits than in the standard approach.

The extent to which the control limits are widened depends on the level of model uncertainty. Table 1 compares the standard ($\pm L\sigma_{z,0}$) and modified ($\pm L\sigma_z$) control limits for various λ, n, $\hat{\phi}$, and $\hat{\theta}$ for ARMA(1, 1) processes. Only positive values of the ARMA parameters were considered, since negative ϕ values result in negative lag one autocorrelation, which is not commonly encountered in industrial processes (Box, et al. [21]). For $\lambda = 0.05$ and $\lambda = 0.1$, the L values that provide a desired in-control ARL of 500 are $L = 2.616$ and $L = 2.814$, respectively (Lucas and Saccucci [20]). As sample size n decreases, model uncertainty increases, and the control limits are widened to a greater extent. This is more apparent from Fig. 1, which shows the relative increase in the control limit width as a function of n and λ, for four different combinations of $\hat{\phi}$ and $\hat{\theta}$. The relative increase r is defined as $r = (\sigma_z - \sigma_{z,0})/\sigma_{z,0}$. The relative increase depends not only on n, but also on λ and the ARMA parameters. For $n = 100$, $\hat{\phi} = 0.95$, and $\hat{\theta} = 0.70$, for example, the relative increase is 15.5% when $\lambda = 0.02$, but only 3.9% when $\lambda = 0.30$. For the same $n = 100$ but with $\hat{\phi} = 0.80$ and $\hat{\theta} = 0.40$, the relative increase becomes 5.1% when $\lambda = 0.02$ and 2.6% when $\lambda = 0.30$.

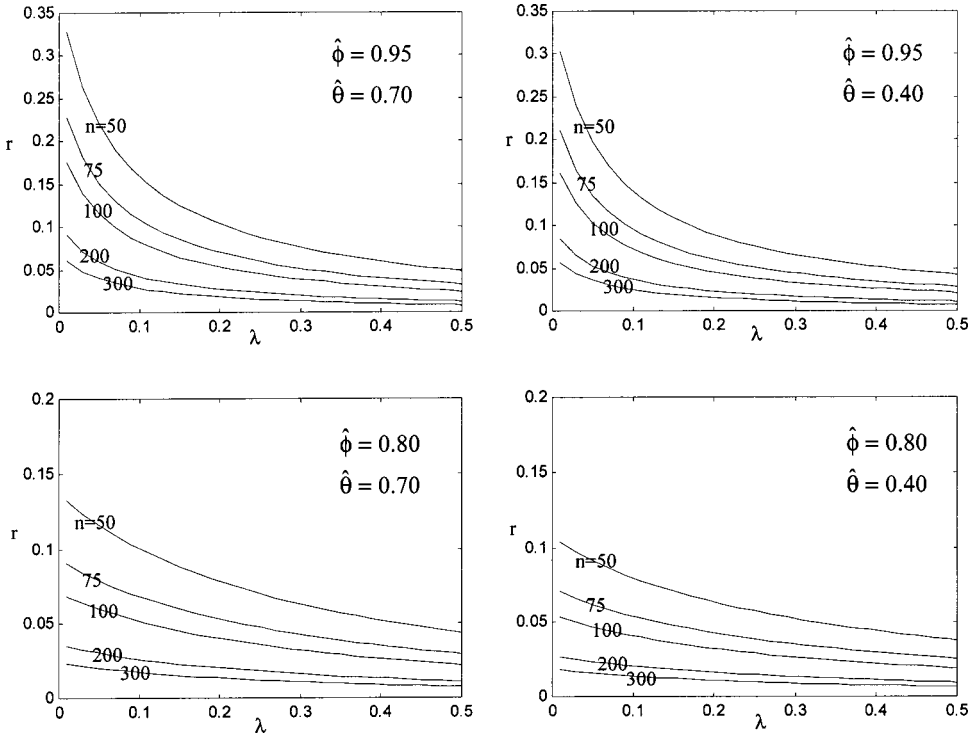

Fig. 1 Relative increase *r* in the EWMA control limits when model uncertainty is considered, for various λ, *n*, $\hat{\phi}$, and $\hat{\theta}$

One question of interest is how large must n be before the relative increase can be considered insignificant, the answer to which depends on λ and the ARMA parameters. For $\lambda = 0.02$, $\hat{\phi} = 0.95$, and $\hat{\theta} = 0.7$, the relative increase does not drop below (say) 5% until $n > 325$. In contrast, for $\lambda = 0.30$ and the same ARMA parameters, the relative increase drops below 5% when $n > 77$. For the limiting case of a Shewhart individual chart ($\lambda = 1.0$), Eq. (16) implies the relative increase is $r = (1 + 2/n)^{1/2} - 1 \cong 1/n$ for all combinations of $\hat{\phi}$ and $\hat{\theta}$. Consequently, for the Shewhart individual chart the relative increase drops below 5% when $n > 20$ and drops below 1% when $n > 100$.

Caution should be used when deciding whether the relative increase is insignificant, since a 5% change in the control limit width can have a large effect on the ARL. Consider a Shewhart individual chart on i.i.d. data $x_t = a_t$ (with no ARMA modeling or modeling errors). Control limits of $\pm 3.09\sigma_a$ result in an in-control ARL of 500 (Montgomery [19]). Control limits of $\pm 2.94\sigma_a$, which are 5% narrower, result in a substantially lower in-control ARL of 305. Control limits of $\pm 3.06\sigma_a$, which are 1% narrower, result in an in-control ARL of 452.

5 Examples and Discussion

The obvious drawback of widening the control limits to safeguard against an undesirably low in-control ARL is that the out-of-control ARL for any size mean shift will inevitably be increased. Since the purpose of control charts is to detect faults as quickly as possible, increases in the out-of-control ARL are undesirable. The following example illustrates this tradeoff, as well as the proposed design procedure for widening the control limits. Consider the concentration readings from the chemical production process represented by series *A* from Box, et al. [21]. Based on these data, the estimated process model is (see Box et al. [21] for details) $x_t - 0.87x_{t-1} = a_t - 0.48a_{t-1}$, where the in-control mean has already been subtracted out of the data. For illustrative purposes, it will be assumed that this is the true model. σ_a^2 is taken to be 1.0 for convenience. 75 additional observations from the process were simulated and used to obtain the parameter estimates $\hat{\phi} = 0.909$, $\hat{\theta} = 0.652$, and $\hat{\sigma}_a^2 = 1.007$.

If $\lambda = 0.05$ ($\nu = 0.95$) and a desired in-control ARL of 500 are chosen, the appropriate L value is 2.616 (from Table 4 of Lucas and Saccucci [20]). From Eq. (16) with the unknown parameters replaced by their estimates, the EWMA variance is

$$\sigma_z^2 \cong \hat{\sigma}_a^2 \left(\frac{1-\nu}{1+\nu} \right) \left[1 + \frac{1+\nu\hat{\phi}}{n(1-\nu\hat{\phi})} + \frac{1+\nu\hat{\theta}}{n(1-\nu\hat{\theta})} \right] = 0.0320,$$

and the modified control limits become $\pm L\sigma_z = \pm 0.468$. In contrast, since $\sigma_{z,0}^2 = \hat{\sigma}_a^2(1-\nu)/(1+\nu) = 0.0258$, the standard control limits are $\pm L\sigma_{z,0} = \pm 0.420$. Thus, to account for model uncertainty the control limits are widened by 11.4%. This has significant impact on the in-control ARL. Monte Carlo simulation with 10,000 replicates reveals that the actual in-control ARL is only 237 using the traditional ± 0.420 control limits. In contrast, when the modified ± 0.468 control limits are used, the actual in-control ARL is 445, much closer to the desired ARL of 500.

As mentioned above, widening the control limits will also increase the out-of-control ARL when a mean shift does occur. To investigate the extent to which the out-of-control ARL is increased, mean shifts of various magnitude μ were added to the process x_t on the initial observation, and Monte Carlo simulation was conducted to estimate the out-of-control ARLs using the standard and modified control limits. 10,000 replicates were conducted for each case. The results are summarized in Table 2. The ARL values for $\mu = 0$ correspond to the in-control ARL. Although the in-control ARL is almost doubled when the modified control limits are used, the out of control ARL is only slightly larger for moderate to large mean shifts. For example, when $\mu = 3.0$ the out-of-control ARLs using the modified and standard control limits are 8.59 and 6.85, respectively.

As discussed in Section 4, the Shewhart individual chart ($\lambda = 1.0$) is much less affected by model uncertainty, to the point that

Table 2 ARL comparison of the standard EWMA, modified EWMA, and Shewhart individual chart for the ARMA(1,1) example in Section 5. The in-control ARL corresponds to a mean shift magnitude $\mu=0$. Control limits for the charts are shown in parentheses.

μ	standard EWMA ($\pm$ 0.420)	modified EWMA ($\pm$ 0.468)	standard Shewhart ($\pm$ 3.101)
0	237	445	450
0.5	132	209	412
1.0	56.4	78.9	322
1.5	28.5	37.4	228
2.0	16.4	21.1	142
2.5	10.3	13.2	78.4
3.0	6.85	8.59	36.6
3.5	4.94	6.03	14.8
4.0	3.78	4.54	5.32
4.5	3.08	3.64	2.00
5.0	2.61	3.03	1.20

widened control limits may not be necessary. Consequently, since the drawback of widening the EWMA control limits is that the out-of-control ARL is increased somewhat, one may speculate that a Shewhart individual control chart with standard control limits would be preferable to an EWMA chart with widened control limits. Table 2, which also shows the ARLs for a Shewhart individual chart with standard control limits ($\pm L\hat{\sigma}_a$ with $L=3.09$), indicates that this is not the case. Even with widened control limits, the EWMA still detects small to moderate size mean shifts much faster that the Shewhart chart. The Shewhart chart only outperforms the EWMA when μ is roughly 4.5 or larger. If one were primarily interested in mean shifts this large, then a Shewhart individual chart would be the best option. For smaller size mean shifts, the EWMA with modified control limits is recommended. Note that the in-control ARL for the Shewhart chart (450) is slightly less than the desired 500. This is because the Shewhart ARL is still affected by modeling errors, albeit by a much lesser extent than the EWMA.

Figure 2 illustrates the differences between the standard EWMA, the modified EWMA, and the Shewhart chart with a typical set of observations from the Monte Carlo simulation. A mean shift of magnitude $\mu=2.5$ was added to the original process x_t on observation number 11. Note that the resulting mean shift in the residuals, which are obtained by filtering x_t via (3), will not simply be a constant mean shift of magnitude μ. Rather, the mean shift in the residuals will be the time-varying function $\hat{\Phi}(B)\hat{\Theta}^{-1}(B)\mu_t$, where μ_t denotes a step function of magnitude μ occurring at time step 11. The time-varying mean of the residuals was referred to as the fault signature in Apley and Shi [6] and the change pattern in Hu and Roan [22], to which the reader is referred for more details. The mean of the residuals gradually decays to the steady-state value $\mu(1-\hat{\phi})/(1-\hat{\theta})=0.65$. This can be seen in the top panel of Fig. 2, which shows the residuals, along with their mean function and the control limits for a Shewhart individual chart. In this case, none of the first 50 residuals exceeded the Shewhart control limits. The bottom panel of Fig. 2

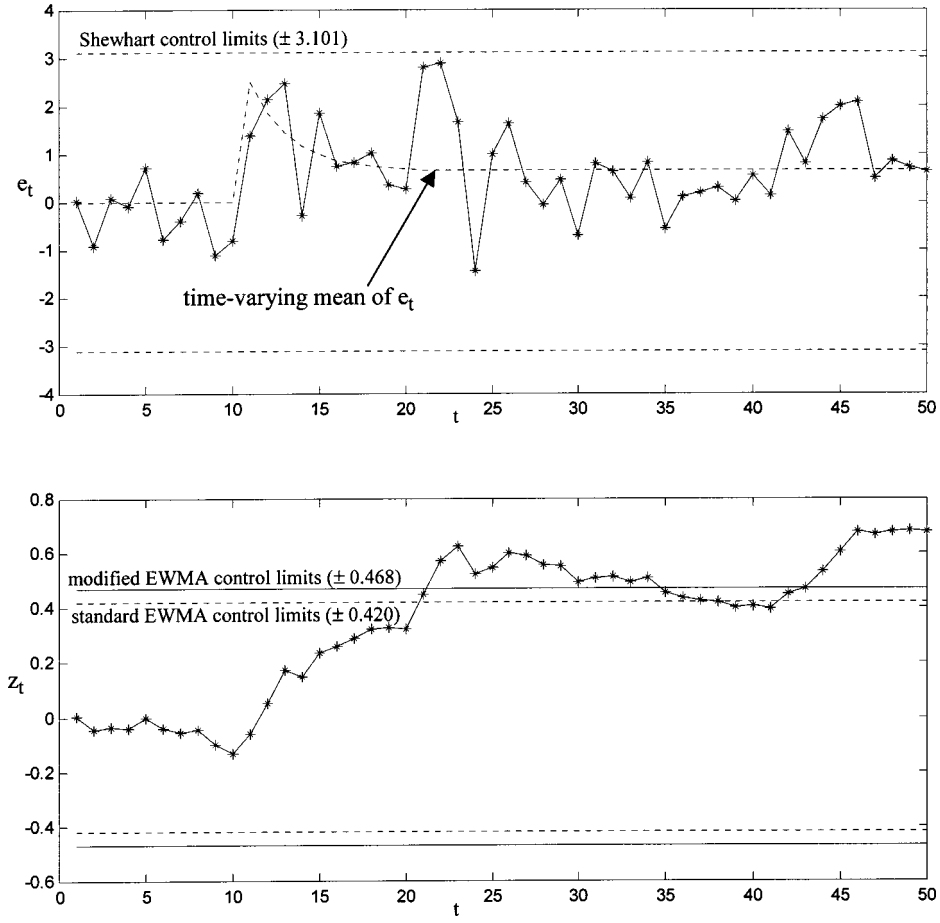

Fig. 2 Residuals e_t and EWMA statistic z_t for the ARMA(1,1) example in Section 5 with a mean shift of magnitude $\mu=2.5$ occurring at observation number 11

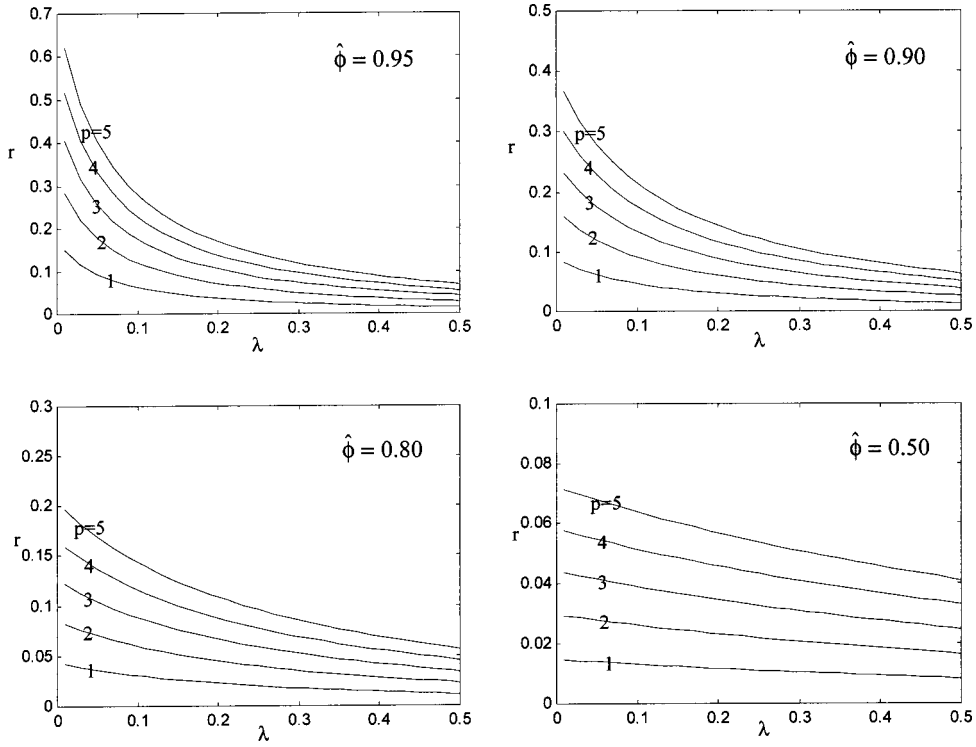

Fig. 3 Relative increase *r* in the EWMA control limits for *p* cascaded AR(1) processes, for various λ, *p*, and $\hat{\phi}$. Sample size is *n*=100 for all cases

shows the EWMA statistic z_t, together with the standard and modified EWMA control limits. The EWMA statistic hovers around zero until the mean shift occurs at observation 11, at which point it gradually climbs towards the upper control limit. The standard EWMA control limit is crossed at observation 21, whereas it takes one additional observation for z_t to cross the modified EWMA control limit.

The preceding discussions centered around first-order ARMA processes. It is reasonable to speculate that since higher-order processes have more parameters that must be estimated, parameter uncertainty will generally be larger and have larger effect on the EWMA variance. This is illustrated in the following example, in which the process is AR(p) and results from a series of p cascaded AR(1) subprocesses. In other words, the output from the i^{th} AR(1) subprocess acts as the input to the $(i+1)^{\text{st}}$ subprocess. The input to the first subprocess is assumed to be white noise, and the output of the p^{th} process is the autocorrelated process x_t to be monitored. This type of cascaded process is common in the chemical and other continuous flow process industries, and is discussed in more detail in English et al. [10]. For illustrative simplicity, we consider the scenario where each of the p subprocesses has the same (estimated) AR(1) parameter $\hat{\phi}$, so that the cascaded AR(p) process is $x_t=(1-\hat{\phi}B)^{-p}a_t$. Figure 3 shows the relative increase r in the EWMA control limit width as a function of λ, for various p and $\hat{\phi}$. The sample size was $n=100$ for all cases, and the method described in Appendix B was used to calculate σ_z for the control limits. From Fig. 3 it is clear that higher-order cascaded processes require a larger relative increase in the control limit width. For $\hat{\phi}=0.95$ and $\lambda=0.05$, for example, the relative increase is 9.3% for $p=1$ and 40.6% for $p=5$. The relative increase also depends strongly on $\hat{\phi}$. For $\hat{\phi}=0.5$ and $\lambda=0.05$, the relative increase drops to 1.4% for $p=1$ and 6.8% for $p=5$.

6. Conclusions

A method has been presented for designing residual-based EWMA control charts for autocorrelated processes when time series process models are estimated with uncertainty. The end result is that the control limits are widened by an amount that depends on the level of model uncertainty, as well as on the choice of EWMA parameter λ. The design method is a relatively straightforward modification of existing methods, in which time series models are assumed perfect. The focus has been on EWMA charts applied to first-order ARMA processes, although results for arbitrary order ARMA processes have also been presented. For the case of first-order ARMA processes, the only information that is needed are the parameter estimates and the number of observations from which the estimates were obtained. For the case of higher-order ARMA processes the parameter covariance matrix is needed, and numerical methods must be used to determine the control limit width.

The extent to which the control limits are widened depends on a number of factors. When sample size and/or the EWMA parameter are large, the relative increase in the control limit width may be quite small. In this case, the standard EWMA control limits should provide an acceptable in-control ARL and it would not be necessary to use the modified control limits. In situations when the sample size is small (e.g., $n<100$) and the EWMA parameter is small (e.g., $\lambda<0.05$), however, the relative increase in the control limit width may be substantial. In these situations, using the widened control limits provides some level of protection against an unacceptably short ARL due to modeling errors.

The obvious drawback of the proposed method is that widening the control limits also increases the out-of-control ARLs, resulting in slower detection of mean shifts. In the example considered in Section 5 the control limits were widened by 11%, resulting in a substantial increase in the in-control ARL (from 237 to 445). The resulting increase in the out-of-control ARL for moderate to large mean shifts was much less dramatic (from 6.85 to 8.59 for a mean shift of size $3\sigma_a$). In this situation, the benefits of using widened control limits would most likely outweigh the disadvantages. Suppose, on the other hand, there had been much larger model uncertainty and the design procedure had called for even wider control limits. The use of excessively widened control limits should be

considered with caution, as the adverse impact on the out-of-control ARLs may be unacceptable. In this situation, a more effective approach may be to collect more data to improve the parameter estimates and reduce model uncertainty. Equation (16) could be used to provide approximate guidelines for how large a sample size is required to have control limits that are widened by not more than (say) 5%.

As a final comment, we point out that the impact of modeling errors is not unique to residual-based charts. For example, if a CUSUM or $\bar{X}$ chart is applied to the original autocorrelated process x_t, the ARL approximations of Johnson and Bagshaw [2] or Vasilopoulos and Stamboulis [3] could be used to suitably widen the control limits. This, however, requires that the parameters of an ARMA process model are known. If the parameters are inaccurate, the resulting modified control limits will also fail to provide the desired ARL. Similar arguments hold if the method of Zhang [23] is used to design an EWMA on x_t. Although an ARMA process model is not explicitly required in Zhang [23], accurate knowledge of the autocorrelation function of x_t is.

Appendix A

This appendix derives the approximate expression for σ_z^2 in Eq. (15) for ARMA(1,1) processes. The impulse response g_j in Eq. (14) is the sum of the impulse responses for the three transfer functions in Eq. (14). That is, $g_j = g_{0,j} - \tilde{\phi} B g_{\phi,j} + \tilde{\theta} B g_{\theta,j} = g_{0,j} - \tilde{\phi} g_{\phi,j-1} + \tilde{\theta} g_{\theta,j-1}$, where $g_{0,j}$, $g_{\phi,j}$, and $g_{\theta,j}$ are defined via

$$\sum_{j=0}^{\infty} g_{0,j} B^j = \frac{1}{1-\nu B} = \sum_{j=0}^{\infty} \nu^j B^j, \tag{A1}$$

$$\sum_{j=0}^{\infty} g_{\phi,j} B^j = \frac{1}{(1-\nu B)(1-\phi B)} = \frac{1}{\nu-\phi} \sum_{j=0}^{\infty} (\nu^{j+1} - \phi^{j+1}) B^j, \text{ and} \tag{A2}$$

$$\sum_{j=0}^{\infty} g_{\theta,j} B^j = \frac{1}{(1-\nu B)(1-\theta B)} = \frac{1}{\nu-\theta} \sum_{j=0}^{\infty} (\nu^{j+1} - \theta^{j+1}) B^j. \tag{A3}$$

Equation (*A*2) follows from equation (3.1.18) of Pandit and Wu [24], by noting that $(1-\nu B)^{-1}(1-\phi B)^{-1}$ is the transfer function for an AR(2) process. Equation (*A*3) follows similarly. Equating coefficients on the left and right sides of Eq. (*A*1) through Eq. (*A*3) to obtain $g_{0,j}$, $g_{\phi,j}$, and $g_{\theta,j}$, and substituting these into $g_j = g_{0,j} - \tilde{\phi} g_{\phi,j-1} + \tilde{\theta} g_{\theta,j-1}$, gives

$$g_j = \nu^j - \frac{\tilde{\phi}(\nu^j - \phi^j)}{\nu-\phi} + \frac{\tilde{\theta}(\nu^j - \theta^j)}{\nu-\theta}, \text{ and}$$

$$E[g_j^2] = \nu^{2j} + \frac{\Sigma_\phi}{(\nu-\phi)^2}(\nu^{2j} - 2\nu^j\phi^j + \phi^{2j}) + \frac{\Sigma_\theta}{(\nu-\theta)^2}(\nu^{2j} - 2\nu^j\theta^j + \theta^{2j}) - \frac{2\Sigma_{\phi\theta}}{(\nu-\phi)(\nu-\theta)}(\nu^{2j} - \nu^j\phi^j - \nu^j\theta^j + \phi^j\theta^j). \tag{A4}$$

Summing Eq. (*A*4) term by term for $j = 0,1,2,\ldots$ gives

$$\sum_{j=0}^{\infty} \nu^{2j} = \frac{1}{1-\nu^2},$$

$$\frac{\Sigma_\phi}{(\nu-\phi)^2} \sum_{j=0}^{\infty} (\nu^{2j} - 2\nu^j\phi^j + \phi^{2j}) = \frac{\Sigma_\phi}{(\nu-\phi)^2(1-\nu^2)} \left[1 - \frac{2(1-\nu^2)}{1-\nu\phi} + \frac{1-\nu^2}{1-\phi^2} \right], \tag{A5}$$

$$\frac{\Sigma_\theta}{(\nu-\theta)^2} \sum_{j=0}^{\infty} (\nu^{2j} - 2\nu^j\theta^j + \theta^{2j}) = \frac{\Sigma_\theta}{(\nu-\theta)^2(1-\nu^2)} \left[1 - \frac{2(1-\nu^2)}{1-\nu\theta} + \frac{1-\nu^2}{1-\theta^2} \right], \text{ and} \tag{A6}$$

$$\frac{2\Sigma_{\phi\theta}}{(\nu-\phi)(\nu-\theta)} \sum_{j=0}^{\infty} (\nu^{2j} - \nu^j\phi^j - \nu^j\theta^j + \phi^j\theta^j) = \frac{2\Sigma_{\phi\theta}}{(\nu-\phi)(\nu-\theta)(1-\nu^2)} \left[1 - \frac{1-\nu^2}{1-\nu\phi} - \frac{1-\nu^2}{1-\nu\theta} + \frac{1-\nu^2}{1-\phi\theta} \right]. \tag{A7}$$

After algebraic manipulation, the terms in brackets in Eq. (*A*5) through Eq. (*A*7) reduce to

$$\left[1 - \frac{2(1-\nu^2)}{1-\nu\phi} + \frac{1-\nu^2}{1-\phi^2} \right] = \frac{(1+\nu\phi)(\nu-\phi)^2}{(1-\nu\phi)(1-\phi^2)}, \tag{A8}$$

$$\left[1 - \frac{2(1-\nu^2)}{1-\nu\theta} + \frac{1-\nu^2}{1-\theta^2} \right] = \frac{(1+\nu\theta)(\nu-\theta)^2}{(1-\nu\theta)(1-\theta^2)}, \text{ and} \tag{A9}$$

$$\left[1 - \frac{1-\nu^2}{1-\nu\phi} - \frac{1-\nu^2}{1-\nu\theta} + \frac{1-\nu^2}{1-\phi\theta} \right] = \frac{(1-\nu^2\phi\theta)(\nu-\phi)(\nu-\theta)}{(1-\nu\phi)(1-\nu\theta)(1-\phi\theta)}. \tag{A10}$$

Substituting Eq. (*A*8) through Eq. (*A*10) into Eq. (*A*5) through Eq. (*A*7), it follows that

$$\sum_{j=0}^{\infty} E[g_j^2] = \frac{1}{1-\nu^2} \left\{ 1 + \frac{\Sigma_\phi}{1-\phi^2} \left[\frac{1+\nu\phi}{1-\nu\phi} \right] + \frac{\Sigma_\theta}{1-\theta^2} \left[\frac{1+\nu\theta}{1-\nu\theta} \right] - \frac{2\Sigma_{\phi\theta}}{1-\phi\theta} \left[\frac{(1-\nu^2\phi\theta)}{(1-\nu\phi)(1-\nu\theta)} \right] \right\}. \tag{A11}$$

Substituting Eq. (*A*11) into Eq. (13) gives the result Eq. (15).

Appendix B

This appendix describes a numerical procedure for calculating σ_z^2 for arbitrary order ARMA models. Similarly to what was done in Appendix A, the impulse response g_j in Eq. (13) can be written as

$$\begin{aligned} g_j &= g_{0,j} + \tilde{\Phi}(B) g_{\phi,j} - \tilde{\Theta}(B) g_{\theta,j} \\ &= g_{0,j} - (\tilde{\phi}_1 B + \tilde{\phi}_2 B^2 + \ldots + \tilde{\phi}_p B^p) g_{\phi,j} + (\tilde{\theta}_1 B + \tilde{\theta}_2 B^2 + \ldots + \tilde{\theta}_q B^q) g_{\theta,j}, \\ &= g_{0,j} - \tilde{\phi}_1 g_{\phi,j-1} - \tilde{\phi}_2 g_{\phi,j-2} - \ldots - \tilde{\phi}_p g_{\phi,j-p} + \tilde{\theta}_1 g_{\theta,j-1} + \tilde{\theta}_2 g_{\theta,j-2} + \ldots + \tilde{\theta}_q g_{\theta,j-q}, \\ &= g_{0,j} + \mathbf{g}_j^T \tilde{\boldsymbol{\gamma}}, \end{aligned} \tag{B1}$$

where $g_{0,j}$, $g_{\phi,j}$, and $g_{\theta,j}$ are defined as the impulse response coefficients of $(1-\nu B)^{-1}$, $(1-\nu B)^{-1}\Phi^{-1}(B)$, and $(1-\nu B)^{-1}\Theta^{-1}(B)$, respectively. The $p+q$ length vector $\mathbf{g}_j$ is defined as $\mathbf{g}_j = [-g_{\phi,j-1} \; -g_{\phi,j-2} \cdots -g_{\phi,j-p} \; g_{\theta,j-1} \; g_{\theta,j-2} \cdots g_{\theta,j-q}]^T$, where it is understood that $g_{\phi,j} = g_{\theta,j} = 0$ for $j < 0$. Thus, from Eqs. (13) and (*B*1),

$$\sigma_z^2 \cong (1-\nu)^2\sigma_a^2\sum_{j=0}^{\infty} E[g_j^2]$$

$$= (1-\nu)^2\sigma_a^2\sum_{j=0}^{\infty} E[(g_{j,0}+\mathbf{g}_j^T\tilde{\boldsymbol{\gamma}})^2]$$

$$= (1-\nu)^2\sigma_a^2\sum_{j=0}^{\infty} E[g_{j,0}^2+2\mathbf{g}_j^T\tilde{\boldsymbol{\gamma}}+\mathbf{g}_j^T\tilde{\boldsymbol{\gamma}}\tilde{\boldsymbol{\gamma}}^T\mathbf{g}_j]$$

$$= (1-\nu)^2\sigma_a^2\sum_{j=0}^{\infty} (\nu^{2j}+\mathbf{g}_j^T\Sigma_\gamma\mathbf{g}_j)$$

$$= \left(\frac{1-\nu}{1+\nu}\right)\sigma_a^2+(1-\nu)^2\sigma_a^2\sum_{j=0}^{\infty}\mathbf{g}_j^T\Sigma_\gamma\mathbf{g}_j, \qquad (B2)$$

where the second to last equality follows from the facts that $g_{0,j} = \nu^j$ and $\tilde{\boldsymbol{\gamma}}$ is zero-mean.

Equation (*B*2) yields a numerical procedure for calculating σ_z^2, given the ARMA parameter estimates and their covariance matrix Σ_γ. To calculate the $\mathbf{g}_j$ vectors, we must substitute the parameter estimates for their unknown true values when calculating the impulse response coefficients $g_{\phi,j}$ and $g_{\theta,j}$ ($j=0,1,2,\ldots$). Numerical procedures for calculating the impulse response coefficients can be found in Pandit and Wu [24] and Box et al. [21]. Since the impulse response coefficients decay exponentially to zero for stable, invertible ARMA models, the summation in (B1) can be truncated to a finite number of terms. Σ_γ is readily available with most ARMA modeling software. Alternatively, the method discussed in Box et al. [21] and Section 2 could be used to calculate Σ_γ.

Nomenclature

x_t = process measurement data, t = time index
a_t = i.i.d. random noise
e_t = time series residuals
z_t = EWMA statistic
ϕ_i = AR parameters
θ_i = MA parameters
p = AR order
q = MA order
σ_a^2 = variance of a_t
σ_z^2 = variance of z_t
$\Phi(B)$ = AR polynomial
$\Theta(B)$ = MA polynomial
B = time series backshift operator
$\hat{}$ = overscore that denotes an estimate of a quantity
$\sim$ = overscore that denotes an estimation error of a quantity
λ = EWMA parameter
ν = $1-\lambda$
L = constant factor in EWMA control limits
$\boldsymbol{\gamma}$ = ARMA parameter vector
Σ_γ = covariance matrix of ARMA parameter estimates
Σ_ϕ = variance of AR parameter estimate
Σ_θ = variance MA parameter estimate
$\Sigma_{\phi\theta}$ = covariance between AR and MA parameter estimates
n = number of observations used to estimate ARMA model
$\sigma_{z|\hat{\gamma}}^2$ = conditional EWMA variance, given $\hat{\gamma}$
g_j = impulse response function of EWMA model

References

[1] Montgomery, D. C., and Woodall, W. H., 1997, "A Discussion on Statistically-Based Process Monitoring and Control," J. Quality Tech. **29**(2), pp. 121–162.
[2] Johnson, R. A., and Bagshaw, M., 1974, "The Effect of Serial Correlation on the Performance of CUSUM tests," Technometrics, **16**(1), pp. 103–112.
[3] Vasilopoulos, A. V., and Stamboulis, A. P., 1978, "Modification of Control Chart Limits in the Presence of Data Correlation," J. Quality Tech., **10**(1), pp. 20–30.
[4] Lu, C. W., and Reynolds, M. R., 1999, "EWMA Control Charts for Monitoring the Mean of Autocorrelated Processes," J. Quality Tech., **31**(2), pp. 166–188.
[5] Alwan, L. C., and Roberts, H. V., 1988, "Time-Series Modeling for Statistical Process Control," Journal of Business and Economic Statistics, **6**(1), pp. 87–95.
[6] Apley, D. W., and Shi, J., 1999, "The GLRT for Statistical Process Control of Autocorrelated Processes," IIE Transactions, **31**(12), pp. 1123–1134.
[7] Berthouex, P. M., Hunter, W. G., and Pallesen, L., 1978, "Monitoring Sewage Treatment Plants: Some Quality Control Aspects," J. Quality Tech., **10**, pp. 139–149.
[8] Dooley, K. J., and Kapoor, S. G., 1990, "An Enhanced Quality Evaluation System for Continuous Manufacturing Processes," Parts 1 and 2, ASME J. Eng. Ind., **112**, pp. 57–68.
[9] Dooley, K. J., Kapoor, S. G., Dessouky, M. I., and DeVor, R. E., 1986, "An Integrated Quality Systems Approach to Quality and Productivity Improvement in Continuous Manufacturing Processes," ASME J. Eng. Ind., **108**, pp. 322–327.
[10] English, J. R., Krishnamurthi, M., and Sastri, T., 1991, "Quality Monitoring of Continuous Flow Processes," Computers and Industrial Engineering, **20**(2), pp. 251–260.
[11] Lin, W. S., and Adams, B. M., 1996, "Combined Control Charts for Forecast-Based Monitoring Schemes," J. Quality Tech., **28**(3), pp. 289–301.
[12] Montgomery, D. C., and Mastrangelo, C. M., 1991, "Some Statistical Process Control Methods for Autocorrelated Data," J. Quality Tech., **23**(3), pp. 179–193.
[13] Notohardjono, B. D., and Ermer, D. S., 1986, "Time Series Control Charts for Correlated and Contaminated Data," ASME J. Eng. Ind., **108**, pp. 219–226.
[14] Runger, G. C., Willemain, T. R., and Prabhu, S., 1995, "Average Run Lengths for Cusum Control Charts Applied to Residuals," Commun. Stat: Theory Meth., **24**(1), pp. 273–282.
[15] Superville, C. R., and Adams, B. M., 1994, "An Evaluation of Forecast-Based Quality Control Schemes," Commun. Stat: Sim. Comp, **23**(3), pp. 645–661.
[16] Vander Wiel, S. A., 1996, "Monitoring Processes That Wander Using Integrated Moving Average Models," Technometrics, **38**(2), pp. 139–151.
[17] Wardell, D. G., Moskowitz, H., and Plante, R. D., 1994, "Run-Length Distributions of Special-Cause Control Charts for Correlated Processes," Technometrics, **36**(1), pp. 3–17.
[18] Adams, B. M., and Tseng, I. T., 1998, "Robustness of Forecast-Based Monitoring Schemes," J. Quality Tech., **30**(4), pp. 328–339.
[19] Montgomery, D. C., 1996, *Introduction to Statistical Quality Control*, 3rd ed., Wiley, New York.
[20] Lucas, J. M., and Saccucci, M. S., 1990, "Exponentially Weighted Moving Average Control Schemes: Properties and Enhancements," Technometrics, **32**(1), pp. 1–12.
[21] Box, G., Jenkins, G., and Reinsel, G., 1994, *Time Series Analysis, Forecasting, and Control*, 3rd ed., Prentice-Hall, Englewood Cliffs, NJ.
[22] Hu, S. J., and Roan, C., 1996, "Change Patterns of Time Series-Based Control Charts," J. Quality Tech., **28**(3), pp. 302–312.
[23] Zhang, N. F., 1998, "A Statistical Control Chart for Stationary Process Data," Technometrics, **40**(1), pp. 24–38.
[24] Pandit, S. M. and Wu, S. M., 1990, "Time Series and System Analysis with Applications," Krieger, Malabar, FL.